Binding interaction of sodium benzoate food additive with bovine serum albumin: multi-spectroscopy and molecular docking studies

Jing Yu[1,2], Jian-Yi Liu[1,2,3], Wei-Ming Xiong[1,2], Xiao-Yue Zhang[1,2]* and Yue Zheng[1,2]*

Abstract

Sodium benzoate (SB) is widely used as a preservative in food industry, and bovine serum albumin (BSA) is a major carrier protein similar to human serum albumin (HSA), the study of the binding between the two has great significance on human health. In this paper, we systematically investigated the binding of SB and BSA under the simulated physiological conditions combining with various common analytical methods, e.g., fluorescence, UV–vis absorption, synchronous fluorescence and circular dichroism (CD) spectra, as well as molecular docking method. The fluorescence quenching measurements were respectively carried out at 298 K, 303 K and 308 K using the Stern–Volmer method. The results reveal that ground state SB–BSA complex was formed within the binding constants from 2.02×10^4 to 7.9×10^3 M^{-1}. Meanwhile, the negative values of ΔH^0 (-43.92 kJ mol^{-1}) and ΔS^0 (-111.6 J mol^{-1} K^{-1}) demonstrated that both the hydrogen binding interaction and van der Waals forces contributed to stabilizing the SB–BSA complex. The site marker competitive experiments show that the SB and BSA bound at site I. Furthermore, the experimental results of UV–vis absorption, synchronous fluorescence and CD spectra indicate that the binding of SB and BSA may change the conformation of BSA. In addition, the molecular docking experiment suggests that hydrogen bond was formed in the interaction between SB and BSA.

Keywords: Sodium benzoate, Bovine serum albumin, Multi-spectroscopy, Molecular docking modeling

Introduction

As a recognized food-grade preservative, sodium benzoate (SB), whose structure is shown in Fig. 1, is widely used in the food, cosmetic, and pharmaceutical industries [1–3]. For example, in the food industry, SB is used in a variety of foods and beverages, such as salads, kimchi, carbonated beverages, jams, juices, and soy sauce, due to its effective inhibition of fungal and bacterial growth during storage [2, 4]. In addition, SB is also applicable in clinically practice and can to treat various diseases, such as urea cycle disorders, liver disease, multiple sclerosis,

and early Alzheimer's disease and Parkinson's disease [5, 6]. Although SB as a preservative is generally recognized as safe (GRAS), its concentration is limited to 0.1% by the US Food and Drug Administration (FDA) [7]. In recent years, studies have shown that the organic form of SB is nontoxic, but its synthetic form is toxic to organisms at chronic doses [8]. Furthermore, it has been reported that SB may damage mitochondrial DNA [9]. Nevertheless, the results of these investigations remain controversial. The interaction between SB and biomacromolecules requires a more in-depth research.

The effect of SB on health can be explored by studying the interaction between SB and Serum albumin (SA). SA, the most abundant translocator protein in blood circulation [10, 11], has several critical physiological functions, for example, the maintenance of the colloidal osmotic blood pressure, and the transportation of various

*Correspondence: zhangxy26@mail.sysu.edu.cn; zhengy35@mail.sysu.edu.cn
[1] State Key Laboratory of Optoelectronic Materials and Technologies, Sun Yat-sen University, Guangzhou 510275, China
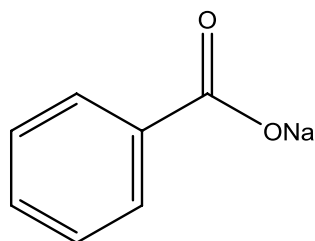Full list of author information is available at the end of the article

Fig. 1 The chemical structure of sodium benzoate (SB)

endogenous and exogenous compounds [12, 13]. Bovine serum albumin (BSA) is not only widely used in bio-medical and pharmaceutical applications, but also widely utilized as a ligand-biological model to study the inter-actions between small molecules and globular proteins, due to its high stability, low-cost, versatile ligand-bind-ing properties, medical importance and high structural homology with human serum albumin (HSA) (approxi-mately 76%) [14, 15]. BSA is a single-chain globular pro-tein consisting of 583 amino acid residues, forming 17 disulfide bonds [16]. In addition, BSA contains two major specific ligand-binding sites located in the hydrophobic cavities in sub-domains II-A and III-A, which are also known as Sudlow's site I and Sudlow's site II, respectively [17]. Meanwhile, previous works have demonstrated that the durability and toxicity of chemicals have huge influence on the structure of BSA because of interaction effect [18]. Moreover, several studies have shown that second-ary structure of BSA changes upon binding with small molecules [19–21]. Therefore, investigating the interac-tion between BSA and chemicals, especially small mol-ecules is of great significance.

In this work, the interaction between SB and BSA was studied by employing multi-spectroscopic methods and molecular docking (MD) modeling. Fluorescence spec-troscopy was first used for understand the binding mech-anism, and quenching mechanism, binding constant, mode and site were analyzed. Then, UV–vis absorp-tion, synchronous fluorescence and CD spectra were employed to determine the conformation and structure of BSA when SB was binding. Furthermore, to further interpret the experimental findings, molecular docking modeling was used to explore the molecular graph of the binding interaction.

Experimental
Chemicals and reagents
All chemicals used in this experiment, including BSA (lyophilized powder, Mw ≈ 66.2 kDa, Sigma) and sodium benzoate (Sinopharm), are of high purity. Thus, no fur-ther purification is required after purchase. PBS buffer

solution (20 mM, pH = 7.40) was prepared with the ultrapure water ($\rho = 18.2$ MΩ cm). Then, BSA solution was prepared using PBS as a solvent for the spectral experiments. Additionally, all solutions were stored in the dark environment with a low temperature of 4 °C before using.

Measurements of the fluorescence spectra
Fluorescence experiments were taken out with the RF-5301 (Shimadzu, Japan) fluorescence spectropho-tometer. Firstly, BSA solution (1×10^{-6} M) was added to a quartz cell with size of 1.0 cm. An equal amount of BSA was added to the reference solution to eliminate the absorbance of BSA itself, and the absorbance of PBS buffer was subtracted through base line correction. Then, SB of different concentrations from 0 to 8×10^{-6} M was gradually dropped into the BSA using a microsyringe. The transportation of various molecules and materials in the blood circulatory system are regulated by albumin. Some of the small molecules entered into the blood are reversibly bound to plasma proteins, forming binding molecules. While those do not bind are free molecules. When the concentration of free molecules decreases, some of the binding molecules dissociate into free mol-ecules, thus, they are always in dynamic equilibrium [22]. In our experiment, SB and BSA were let stand for 5 min to reach dynamic equilibrium [23]. During the fluorescence measurement, the slit width was set at 10 nm/10 nm, the excitation wavelength was 285 nm, and the scanning range of the fluorescence emission spec-trum was 300–450 nm.

Measurements of the synchronous fluorescence
The synchronous fluorescence of SB–BSA was measured using the same concentrations of the mixture solutions as in the fluorescence quenching measurements, but at room temperature. Spectra were recorded at Δλ = 15 nm and 60 nm, which showed the tyrosine residue and tryp-tophan residue characteristics of the BSA.

Measurements of UV–vis spectra
The UV–vis absorption spectra were obtained by a UV-3600 (Shimadzu, Japan) spectrophotometer. The con-centration of BSA was kept at 1×10^{-6} M, while the con-centration of the added SB ranged from 0 to 8×10^{-6} M, each time with an increase of 2×10^{-6} M. The absorp-tion spectra of the BSA between 230 and 330 nm were recorded in a 1 cm quartz absorption cell.

Measurements of CD spectra
CD spectra were recorded using the spectropolarimeter of JASCO J-810 and a 1.0 cm quartz absorption cell. Note that the spectrum of a cell only with PBS buffer solution

Yu *et al. BMC Chemistry* (2019) 13:95

Page 3 of 8

was firstly measured as background signal to remove the influence of PBS buffer solution.

Molecular docking

Molecular docking simulation was employed to study the molecular interaction between BSA and SB using Auto Dock Vina, an open-source software with significantly fast dock running speed and high molecular docking accuracy [24]. To prepare the protein and ligand molecules for docking study, BSA crystal structure was first retrieved from the Protein Data Band (PDB ID: 3V03) (http://www.rcsb.org/structure/3V03), and then loaded on AutoDock Tools to remove additional molecules, e.g., all the water molecules. Next, Polar hydrogens and Gasteiger charges were added, respectively. The structure of SB was prepared by drawing the 2D chemical structure using ChemOffice and further optimized based on MM2 force field implemented using Chem3D. After that, the structurally optimized BSA and SB were employed to conduct molecular docking simulation. During the simulation, the size of the grid box along x-, y- and z-directions were all set at 18 Å and the grid spacing 1 Å. The grid box center was set at (88.537, 24.797, 13.111). The energy range and values were set at 4 kcal/mol and 100, respectively.

Results and discussion

Fluorescence spectral analysis of the interactions involving SB with BSA

Fluorescence quenching of BSA

Tryptophan (Trp), tyrosine (Tyr) and phenylalanine (Phe) residues are three main amino acids that can make protein generate endogenous fluorescence [25]. The major contribution to the changed fluorescence of BSA is from the environmentally-sensitive tryptophan (Trp) moiety [26]. The fluorescence emission spectra of BSA with various concentration of SB are shown in Fig. 2a. When excited at 285 nm, BSA had a characteristic band at around 344 nm. Furthermore, when the concentration of the added SB increased from 0 to 8×10^{-6} M, the fluorescence intensity of BSA decreased significantly, indicating that the environment around the Trp residues of BSA varied with the addition of SB. Therefore, it can be inferred that there is a binding interaction between SB and BSA, and the binding site is located near the Trp residue [27].

The reaction temperatures for SB–BSA system were maintained at 298 K, 303 K, and 308 K, respectively. The fluorescence quenching data are analyzed by the Stern–Volmer equation [28]:

$$\frac{F_0}{F} = 1 + K_{SV}[Q] = 1 + k_q \tau_0 [Q] \tag{1}$$

where F and F_0 are the fluorescence intensity of BSA with and without the quencher, i.e., SB, respectively. K_{SV} is the Stern–Volmer quenching constant with the unit being M^{-1}, and $[Q]$ is the concentration of the quencher. k_q is the quenching rate constant of BSA. τ_0 is the average fluorescence lifetime of BSA in the excited state without the quencher (the order of magnitude is 10^{-8}) [28]. K_{SV} and K_q value of BSA triggered by SB at different temperatures can be determined by calculating the slope of the curve, as shown in Fig. 2b. The values of the parameters K_{SV}, k_q and R at different temperatures are listed in Table 1. It can be seen from the results that K_{SV} decreases from 1.87×10^4 to 1.34×10^4 M^{-1} as the temperature increases from 298 to 308 K. Moreover, the values of k_q at various temperatures are all in the order of 10^{12} $M^{-1}\,s^{-1}$, which
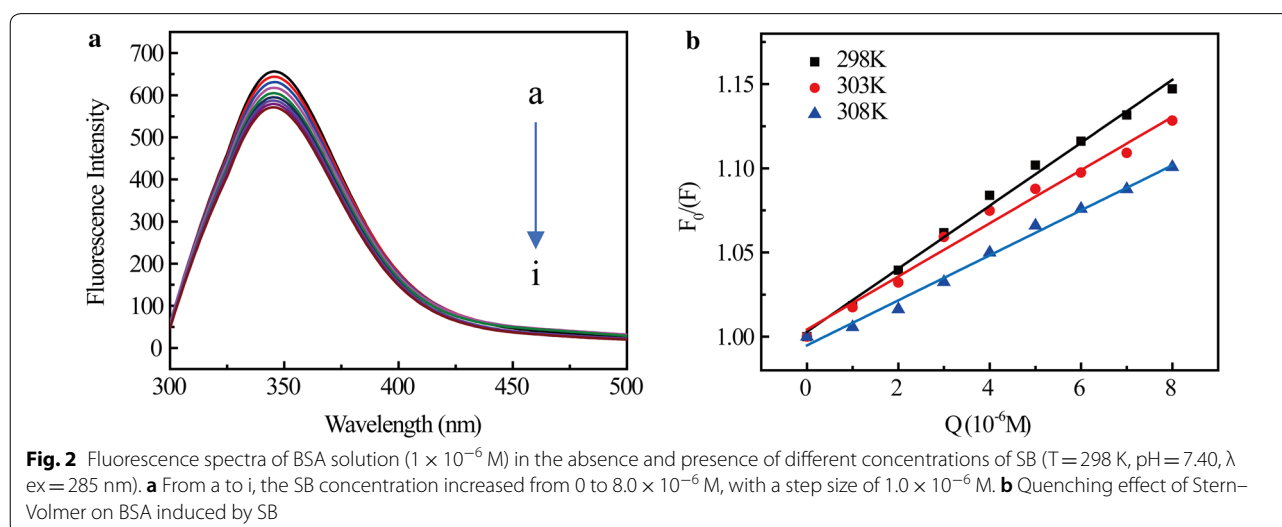

Fig. 2 Fluorescence spectra of BSA solution (1×10^{-6} M) in the absence and presence of different concentrations of SB (T = 298 K, pH = 7.40, λ ex = 285 nm). **a** From a to i, the SB concentration increased from 0 to 8.0×10^{-6} M, with a step size of 1.0×10^{-6} M. **b** Quenching effect of Stern–Volmer on BSA induced by SB

Table 1 Stern–Volmer Constants of Stern-Volmer quenching (K_{SV}) and bimolecular quenching rate (K_q) at tested temperatures

T (K)	K_{SV} (10^4 M^{-1})	K_q (10^{12} M^{-1} S^{-1})	R
298	1.87	1.87	0.99327
303	1.58	1.58	0.99302
308	1.34	1.34	0.99579

R represents correlation coefficient

are much larger than the maximum diffusion collision quenching rate constant (2.0×10^{10} M^{-1} s^{-1}), indicating that the SB-trigger BSA quenching process is static rather than dynamic.

Interaction parameters and binding model for SB–BSA complex

The binding constants (K_b) and binding site (n) of SB–BSA complex is calculated using the following formula [29]:

$$\lg \frac{(F_0 - F)}{F} = \lg K_b + n \lg [Q] \tag{2}$$

According to the Eq. (2), K_b and n can be calculated from the curve of $\log[(F_0-F)/F]$ versus $\log[Q]$, as shown

in Fig. 3a. The calculated results are summarized in Table 2. These results show that within the temperature range studied, the value n of SB–BSA complex is close to 1, indicating that BSA has a single high affinity binding site for SB. K_b is calculated to be approximately 10^4, indicating strong binding interactions between SB and BSA. It is also found that as temperature increases, K_b value decreases, suggesting that the stability of SB–BSA complex decreases with the increasing of temperature.

To better understand the binding between BSA and SB, the van't Hoff Eq. (3) was used to calculate the thermodynamic enthalpy (H_0) and entropy (S_0) of BSA and SB complexation.

$$\ln K_b = -\frac{\Delta H^0}{RT} + \frac{\Delta S^0}{R} \tag{3}$$

As shown in Fig. 3b, the curves of $\ln K_b$ and $1/T$ were used to determine the thermodynamic parameters of SB–BSA complex at three different temperatures, i.e. 298 K, 303 K, and 308 K. Once the H_0 and S_0 values are determined, the variation in Gibbs free energy (G_0) can be calculated by the following standard Eq. (4).

$$\Delta G^0 = \Delta H^0 - T\Delta S^0 \tag{4}$$

Here, the binding constant values at three different temperatures, i.e. ΔG_0, ΔH_0 and ΔS_0, are listed in Table 2.
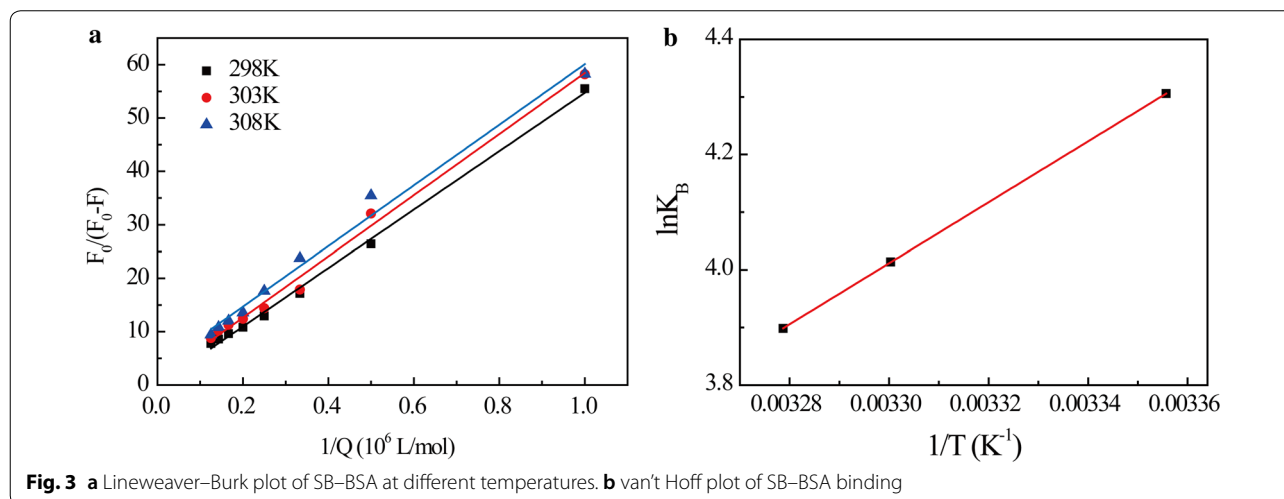

Fig. 3 **a** Lineweaver–Burk plot of SB–BSA at different temperatures. **b** van't Hoff plot of SB–BSA binding

Table 2 Calculated parameters of SB–BSA complex at different testing temperatures at pH 7.4

T(K)	K_b (10^4 M^{-1})	n	R	ΔG^0 (KJ/mol)	ΔS^0 (J mol^{-1} K^{-1})	ΔH^0 (KJ/mol)
298	2.02	1.00	0.9973	− 9.35	− 111.6	− 43.92
303	1.03	0.96	0.9933	− 8.78	− 111.6	− 43.92
308	0.79	0.95	0.9971	− 8.12	− 111.6	− 43.92

K_b, n, G^0, S^0 and H^0 are binding constant, binding site, Gibbs free energy, thermodynamic enthalpy and entropy, respectively. R represents correlation coefficient

Yu *et al. BMC Chemistry*   (2019) 13:95

Page 5 of 8

The negative value of ΔG_0 indicates that the interaction process between SB and BSA is spontaneous. And the positive H_0 and S_0 values indicate that hydrogen bonding and van der Waals interactions play a major role in the binding of the chemical to the protein [30, 31].

Combination of fluorescent probes

To determine the displacement percentage of the fluorescent combination probe, according to the method introduced by Sudlow et al., the fluorescence markers for distinct binding sites were chosen: ketoprofen for site I and ibuprofen for site II [32]. And the following equation is also adopted.

$$\text{Probe displacement } (\%) = F_2/F_1 \times 100 \qquad (5)$$

where F_1 and F_2 represent the fluorescence intensity of the SB–BSA system in the absence and presence of the probe, respectively. As shown in Fig. 4. The increase in ketoprofen concentration results in significant decrease in the fluorescence intensity of the SB–BSA system. However, the increase in ibuprofen concentration has little impact on the fluorescence intensity of BSA. Therefore, SB and BSA are supposed to bind at site I [33].

Conformational change of BSA

Analysis of the UV–visible absorption spectra

UV absorption measurement, a very simple and effective method, is often used to observe the formation process and the change in the conformation of protein during the its binding interaction between with small molecule. The UV spectra of SB–BSA complex are shown in Fig. 5. All SB–BSA complex have absorption bands. The absorption band around 280 nm is the result of the π−π* transition of aromatic amino acids (Trp, Tyr, and Phe) [34]. Adding
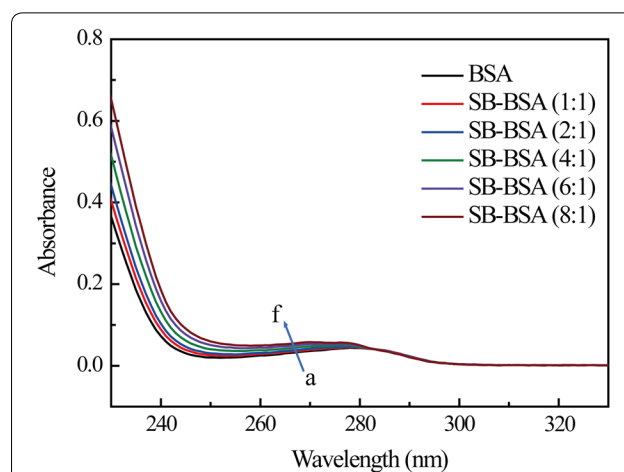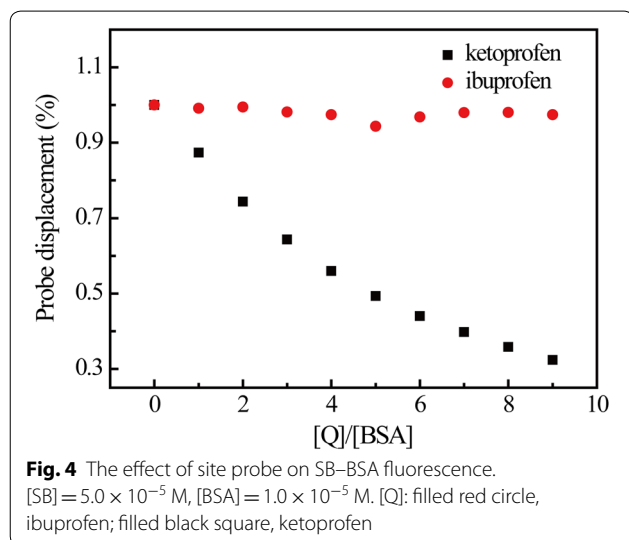

Fig. 4 The effect of site probe on SB–BSA fluorescence. [SB] = 5.0×10^{-5} M, [BSA] = 1.0×10^{-5} M. [Q]: filled red circle, ibuprofen; filled black square, ketoprofen

Fig. 5 The UV–Vis absorption spectra of BSA in the absence and presence of different concentrations of SB. The BSA concentration was 1.0×10^{-6} M; while the SB concentration increased from 0 to 8.0×10^{-6} M, with a step size of 2.0×10^{-6} M from a to f

SB (0–8.0×10^{-6} M) to the BSA solution enhances the absorption intensity (0.044–0.0556), and the maximum wavelength shows a slight blue shift at around 280 nm. The UV absorption intensity increases with the increase of SB concentration, indicating that complex is formed by SB and the amino acid residues of BSA.

Synchronous fluorescence spectroscopy

The synchronous fluorescence spectroscopy is a useful tool for obtaining information around chromophore microenvironment. Usually, the shift of the λem represents the alteration of the polarity of the amino acid environment (particularly Tyr or Trp residues) [35]. The synchronous fluorescence spectra were carried out for investigating structural change in BSA with SB addition (Fig. 6). The fluorescence spectra characteristic of tyrosine and tryptophan residues are shown in Fig. 6a ($\Delta\lambda = 15$ nm) and Fig. 6b ($\Delta\lambda = 60$ nm), respectively [36]. It is obvious that the fluorescence intensity of the tryptophan residues are much stronger than that of tyrosine residues in Fig. 6. And no significant change is found in the fluorescent emission peak position of both tyrosine and tryptophan residues. Thus, the addition of SB did not rearrange the microenvironment of the tyrosine and tryptophan residues in BSA.

Analysis of CD spectra

To further explore whether SB can induce conformational change in BSA, CD spectroscopy experiments were performed. The two negative bands at 208 nm (π−π*
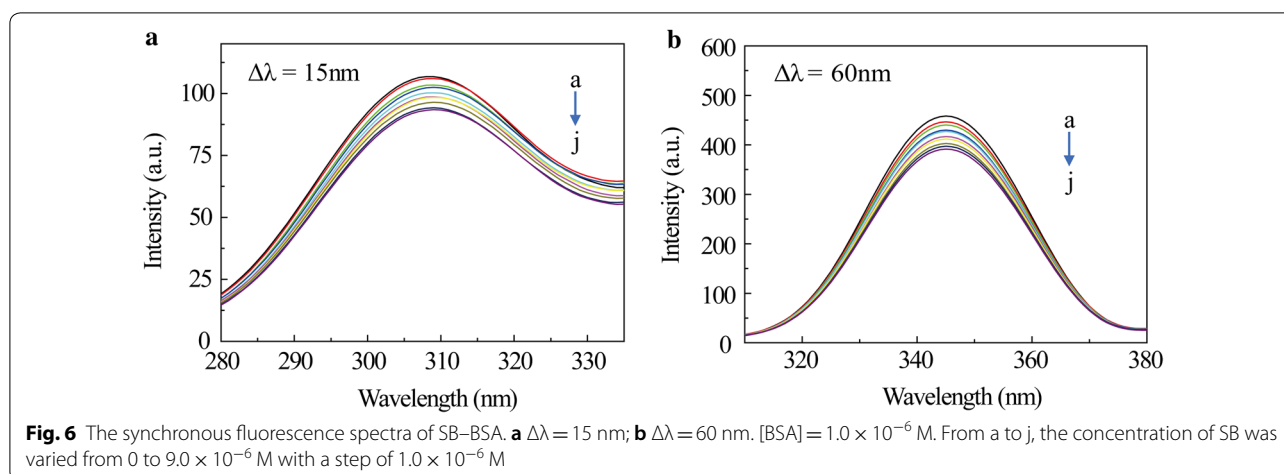
Fig. 6 The synchronous fluorescence spectra of SB–BSA. **a** $\Delta\lambda = 15$ nm; **b** $\Delta\lambda = 60$ nm. [BSA] $= 1.0 \times 10^{-6}$ M. From a to j, the concentration of SB was varied from 0 to 9.0×10^{-6} M with a step of 1.0×10^{-6} M

transition) and 222 nm (n-π* transition) in CD spectrum of free BSA are characteristic of the protein α-helical structure [37], whose content can be estimated by [38]:

$$\text{a-helix (\%)} = [(-\text{MRE}_{208} - 4000) / (33000 - 4000)] \times 100 \quad (6)$$

where MRE_{208} is the MRE value observed at 208 nm, 4000 is the MRE value of the β shape and random coil conformation at 208 nm, and 33000 is the MRE value of the pure α-helix at 208 nm. The MRE_{208} value used to indicate the change in secondary structure of BSA determined by [38]:

$$\text{MRE}_{208} = CD(\text{m deg})_{208}/(10 \times n \times l \times C_p) \quad (7)$$

where n is the number of amino acid residues (583 for BSA). l is the cell path length, and C_p is the molar concentration of BSA. When SB:BSA ratio increases from 0 to 2:1, the band intensities of the CD spectra have a slight decrease, whereas the peaks positions remain unchanged, as shown in Fig. 7. The results demonstrate that the secondary structure of BSA has a partial change from α-helical content. The α-helical content decreased from 62.7% of free BSA to 61.88% (SB:BSA = 1:1) and 60.24% (SB:BSA = 2:1). Based on these analyses, we conclude that the addition of SB alters the secondary structure of BSA, resulting in a decrease in α-helical content, which is nonetheless still dominant in the secondary structure.

Molecular docking

To further elucidate SB–BSA binding interaction, molecular docking was used to simulate the molecular interaction between BSA and SB. The simulated result of the predominate configuration of SB–BSA complex is plotted in Fig. 8, where the binding energy is the lowest. Moreover, as shown in Fig. 9, the binding results indicate that SB is very close to the amino acid residues Tyr149, Leu237, Arg256, Leu259, Ala260, Ile263, Ser286, Ile289,
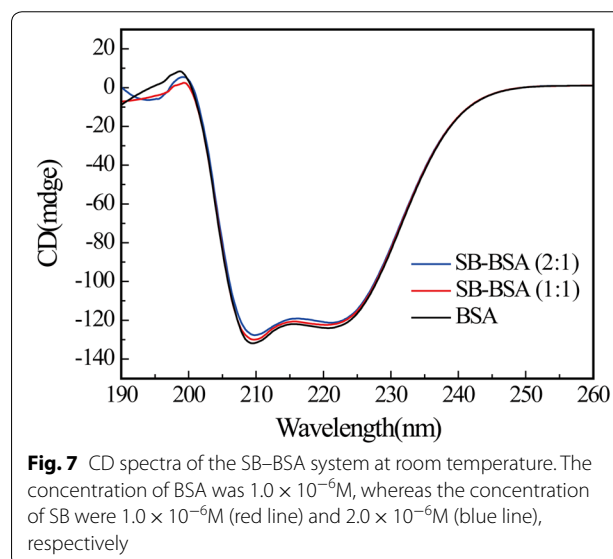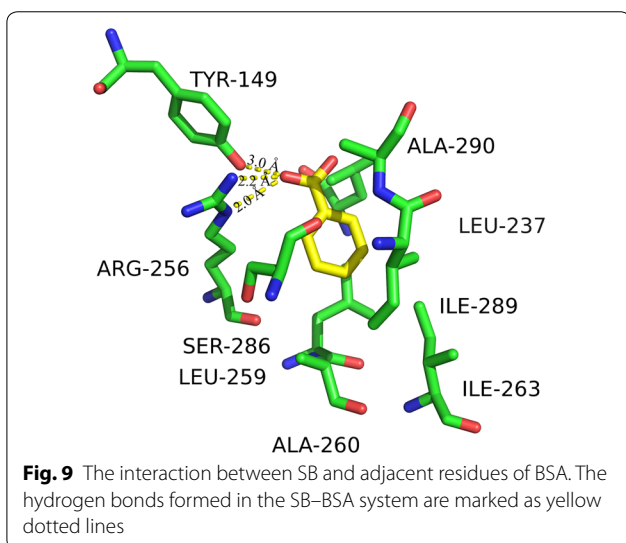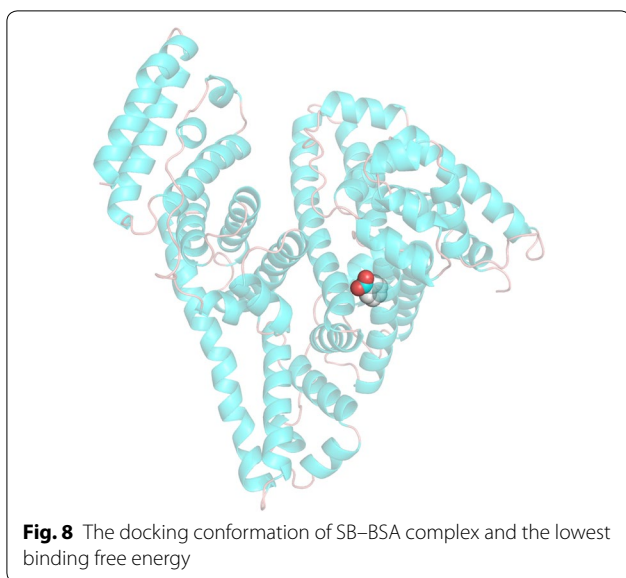

Fig. 7 CD spectra of the SB–BSA system at room temperature. The concentration of BSA was 1.0×10^{-6} M, whereas the concentration of SB were 1.0×10^{-6} M (red line) and 2.0×10^{-6} M (blue line), respectively

and Ala290 at site I in subdomain IIA. The hydrogen bonding between SB and BSA (Tyr149, ARG256 with a bond length of 3.0 Å, 2.2 Å and 2.0 Å) is also responsible for maintaining the stability of the complex. Here, note that the calculated combined Gibbs free energy is −5.7 kcal/mol (−23.8 kJ/mol) and binding constant (K_b) is about 1.45×10^4 mol/L, which is quite different with our experimental result ($\Delta G = -935$ kJ/mol and $K_b = 2.2 \times 10^4$ mol/L). This may be caused by the difference between X-ray crystal structure of BSA and its solution state in the aqueous system.

Conclusion

In this study, we combined the multi-spectroscopic methods and molecular docking modeling to systematically investigate the interaction between SB and BSA.

Yu *et al. BMC Chemistry*   (2019) 13:95

Page 7 of 8

Fig. 8 The docking conformation of SB–BSA complex and the lowest binding free energy

Fig. 9 The interaction between SB and adjacent residues of BSA. The hydrogen bonds formed in the SB–BSA system are marked as yellow dotted lines

The multi-spectroscopic data show that the quenching of BSA binding with SB was caused by the formation of SB–BSA complex. The negative values of ΔH^0 and ΔS^0 demonstrated that hydrogen bonding and van der Waals forces contribute to make the SB–BSA complex stable. The negative values of ΔG indicate that the interaction process was spontaneous. Site marker competitive experiments show that SB and BSA bound at site I. In addition, the amino acid microenvironments and the secondary structure of BSA were altered by the addition of SB, as shown in UV–vis absorption, synchronous fluorescence spectroscopy and CD spectra data. Furthermore, molecular docking studies provided some valuable information

on the interaction between SB and BSA and structural stability of their complex.

Author details

[1] State Key Laboratory of Optoelectronic Materials and Technologies, Sun Yat-sen University, Guangzhou 510275, China. [2] Micro&Nano Physics and Mechanics Research Laboratory, School of Physics, Sun Yat-sen University, Guangzhou 510275, China. [3] Sino-French Institute of Nuclear Engineering and Technology, Sun Yat-sen University, Zhuhai 519082, China.

References

1. Baranowska I, Wojciechowska I, Solarz N et al (2013) Determination of preservatives in cosmetics, cleaning agents and pharmaceuticals using fast liquid chromatography. J Chromatogr Sci 52(1):88–94
2. Lennerz B-S, Vafai S-B, Delaney N-F, Clish A-B, Pierce K-A, Ludwig D-S, Mootha V-K (2015) Effect of sodium benzoate, a widely used food preservative, on glucose homeostasis and metabolic profiles in humans. Mol Genet Metab 114(1):73–79
3. Ikarashi Y, Uchino T, Nishimura T (2010) Analysis of preservatives used in cosmetic products: salicylic acid, sodium benzoate, sodium dehydroacetate, potassium sorbate, phenoxyethanol, and parabens. Bull Natl Inst Health Sci 128:85–90
4. Nettis E, Colanardi M-C, Ferrannini A et al (2004) Sodium benzoate-induced repeated episodes of acute urticaria/angio-oedema: randomized controlled trial. Br J Dermatol 151(4):898–902
5. Yavav A, Kumar A, Das M, Tripathi A (2016) Sodium benzoate, a food preservative, affects the functional and activation status of splenocytes at non cytotoxic dose. Food Chem Toxicol 88:40–47
6. Häberle J, Boddaert N, Burlina A, Chakrapani A, Dixon M, Huemer M, Karall D, Martinelli D, Crespo P-S, Santer R, Servais A, Valayannopoulos V, Lindner M, Rubio V, Dionisi-Vici C (2012) Suggested guidelines for the diagnosis and management of urea cycle disorders. Orphanet J Rare Dis 7(1):32

Yu *et al. BMC Chemistry*   (2019) 13:95

Page 8 of 8

7.   Misel M-L, Gish R-G, Patton H, Mendler M, Pahan K (2011) Immunomodu-lation of experimental allergic encephalomyelitis by cinnamon metabo-lite sodium benzoate. Immunopharmacol Immunotoxicol 33(4):586–593

8.   Kehinde O-S, Christianah O-I, Oyetunji O-A (2018) Ascorbic acid and sodium benzoate synergistically aggravates testicular dysfunction in adult Wistar rats. Int J Physiol Pathophysiol Pharmacol 10(1):39

9.   Piper J-D, Piper P-W (2017) Benzoate and sorbate salts: a systematic review of the potential hazards of these invaluable preservatives and the expanding spectrum of clinical uses for sodium benzoate. Compr Rev Food Sci F 16(5):868–880

10. Zhang Q, Ni Y, Kokot S (2016) Competitive interactions between glu-cose and lactose with BSA: which sugar is better for children? Analyst 141(7):2218–2227

11. Leblanc A, Shiao T-C, Roy R, Sleno L (2014) Absolute quantitation of NAPQI-modified rat serum albumin by LC-MS/MS: monitoring acetami-nophen covalent binding in vivo. Chem Res Toxicol 27(9):1632–1639

12. Sharifi M, Dolatabadi JEN, Fathi F et al (2017) Kinetic and thermodynamic study of bovine serum albumin interaction with rifampicin using surface plasmon resonance and molecular docking methods. J Biomed Opt 22(3):037002

13. Janek T, Czyżnikowska Ż, Łuczyński J et al (2017) Physicochemical study of biomolecular interactions between lysosomotropic surfactants and bovine serum albumin. Colloids Surf B 159:750–758

14. Mote U-S, Bhattar S-L, Patil S-R (2010) Interaction between felodipine and bovine serum albumin: fluorescence quenching study. J Lumin 25(1):1–8

15. Shama Y, Riyazuddeen (2017) Exploring thermodynamic parameters and the binding energetic of berberine chloride to bovine serum albumin (BSA): spectroscopy, isothermal titration calorimetry and molecular dock-ing techniques. Thermochim Acta 655:76–78

16. Chaturvedi S-K, Ahmad E, Khan J-M, Alam P, Ishtikhar M, Khan R-H (2015) Elucidating the interaction of limonene with bovine serum albumin: a multi-technique approach. Mol Bio Syst 11(1):307–316

17. Guan J, Yan X, Zhao Y-J, Sun Y-H, Peng X (2018) Binding studies of triclo-carban with bovine serum albumin: insights from multi-spectroscopy and molecular modeling methods. Spectrochim Acta A 202:1–12

18. Shi JH, Zhou KL, Lou YY, Pan DQ (2018) Multi-spectroscopic and molecu-lar modeling approaches to elucidate the binding interaction between bovine serum albumin and darunavir, a HIV protease inhibitor. Spectro-chim Acta A 188:362–371

19. Skrt M, Benedik E, Podlipnik C, Poklar Ulrih N (2012) Interactions of differ-ent polyphenols with bovine serum albumin using fluorescence quench-ing and molecular docking. Food Chem 135(4):2418–2424

20. Tian J, Liu J, He W, Hu Z, Yao X, Chen X (2004) Probing the binding of scutellarin to human serum albumin by circular dichroism, fluorescence spectroscopy, FTIR, and molecular modeling method. Biomacromol 5(5):1956–1961

21. Makarska-Bialokoz M (2017) Investigation of the binding affinity in vitamin B12-Bovine serum albumin system using various spectroscopic methods. Spectrochim Acta A 184:262–269

22. Agarwal R-P, Phillips M, McPherson R-A et al (1986) Serum albumin and the metabolism of disulfiram. Biochem Pharmacol 35(19):3341–3347

23. Zhang J, Li WX, Ao BY et al (2014) Fluorescence enhancement of euro-pium (III) perchlorate by benzoic acid on bis (benzylsulfinyl) methane complex and its binding characteristics with the bovine serum albumin (BSA). Spectrochim Acta A 118:972–980

24. Trott O, Olson A-J (2010) AutoDock Vina: improving the speed and accu-racy of docking with a new scoring function, efficient optimization, and multithreading. J Comput Chem 31(2):455–461

25. Lou Y-Y, Zhou K-L, Pan D-Q et al (2017) Spectroscopic and molecular docking approaches for investigating conformation and binding charac-teristics of clonazepam with bovine serum albumin (BSA). J Photochem Photobiol B 167:158–167

26. Sandhya B, Hegde A-H, Kalanur S-S et al (2011) Interaction of triproli-dine hydrochloride with serum albumins: thermodynamic and binding characteristics, and influence of site probes. J Pharm Biomed Anal 54(5):1180–1186

27. Shen G-F, Liu T-T, Wang Q, Jiang M, Shi J-H (2015) Spectroscopic and molecular docking studies of binding interaction of gefitinib, lapatinib and sunitinib with bovine serum albumin (BSA). J Photochem Photobiol B 153:380–390

28. Zhao L-Z, Liu R-T, Zhao X-C, Yang B-J, Gao C-Z, Hao X-P et al (2009) New strategy for the evaluation of CdTe quantum dot toxicity targeted to bovine serum albumin. Sci Total Environ 407(18):5019–5023

29. Safarnejad A, Shaghaghi M, Dehghan G, Soltani S (2016) Binding of carvedilol to serum albumins investigated by multi-spectroscopic and molecular modeling methods. J Lumin 176:149–158

30. Ross P-D, Subramanian S (1981) Thermodynamics of protein association reactions: forces contributing to stability. Biochemistry 20(11):3096–3102

31. Xu X-Y, Du Z-Y, Wu W-H, Wang Y-F, Zhang B, Mao X-Y, Jiang L, Yang J, Hou S-F (2017) Synthesis of triangular silver nanoprisms and spectroscopic analysis on the interaction with bovine serum albumin. Anal Bioanal Chem 409(22):5327–5336

32. Yao D, Yu J, Pan Y-M, Huang F-P, Bian H-D, Yu Q, Liang H, Chen Z-F (2012) Spectroscopic studies on the binding of kaempferol-3,7-α-ʟ-rhamnopyranoside to bovine serum albumin. Chin J Chem 30(2):438–444

33. Zhang G-W, Ma Y-D (2013) Mechanistic and conformational studies on the interaction of food dye amaranth with human serum albumin by multispectroscopic methods. Food Chem 136(2):442–449

34. Chi Z-X, Liu R-T, Teng Y, Fang X-Y, Gao C-Z (2010) Binding of oxytetracy-cline to bovine serum albumin: spectroscopic and molecular modeling investigations. J Agric Food Chem 58(18):10262–10269

35. Ghosh K, Rathi S, Arora D (2016) Fluorescence spectral studies on interac-tion of fluorescent probes with Bovine Serum Albumin (BSA). J Lumin 175:135–140

36. Abert W-C, Gregory W-M, Allan G-S (1993) The binding interaction of Coomassie blue with proteins. Anal Biochem 213(2):407–413

37. Yasmeen S, Riyazuddeen (2017) Biophysical insight into the binding of triprolidine hydrochloride to human serum albumin: calorimetric, spec-troscopy and molecular docking approaches. J Mol Liq 233:55–63

38. Shi J-H, Chen J, Wang J, Zhu Y-Y, Wang Q (2015) Binding interaction of sorafenib with bovine serum albumin: spectroscopic methodologies and molecular docking. Spectrochim Acta A 149:630–637

Publisher's Note